Utilization of Multipaths for Spread-Spectrum Code Acquisition in Frequency-Selective Rayleigh Fading Channels

Oh-Soon Shin, *Student Member, IEEE,* and Kwang Bok (Ed) Lee, *Member, IEEE*

***Abstract*—A novel acquisition scheme that utilizes multipaths to improve acquisition performance is proposed for frequency-selective fading channels. The proposed acquisition scheme employs nonconsecutive search and joint triple-cell detection. The performance is analyzed in frequency-selective Rayleigh fading channels. Equations for the probabilities of detection and false alarm are derived, and an expression for the mean acquisition time is developed. The mean acquisition time performance of the proposed and conventional acquisition schemes is evaluated and compared. It is found that the proposed acquisition scheme significantly outperforms the conventional one. The effects of various channel parameters such as the number of resolvable paths, the shape of the multipath intensity profile (MIP) and the signal-to-interference ratio (SIR) on acquisition performance are also investigated.**

***Index Terms*—Acquisition, frequency-selective Rayleigh fading, joint triple-cell detection, nonconsecutive search, spread-spectrum.**

I. Introduction

DIRECT-SEQUENCE spread-spectrum (DS/SS) has attracted considerable interest in commercial applications and has been chosen for next generation mobile radio systems [1], [2]. In DS/SS systems, code synchronization is important because data demodulation is possible only after synchronization is performed. The code synchronization is usually achieved in two steps: acquisition for coarse alignment and tracking for fine alignment, of which the former is addressed in this paper.

Various acquisition schemes have been investigated for rapid acquisition, which may be classified into either serial search or parallel search. Cells in an uncertainty region are consecutively tested in a serial search, and it is widely employed due to simple implementation. In [3], a serial search scheme has been discussed and mean acquisition time performance has been analyzed in a static channel. The analysis has been extended to frequency-selective Rayleigh fading channels in [4]. In a parallel search, cells are simultaneously tested, and the use of parallel search is desirable in applications where faster acquisition is required at the cost of complexity. The performance of the parallel acquisition scheme is extensively analyzed in static and fading channels [5]–[8].

In frequency-selective fading channels where delay spread is greater than the chip duration, there exist a number of resolvable paths. From the viewpoint of acquisition, the existence of multipaths implies that there exist more than one in-phase cells. The in-phase cell is defined as a cell where the timing error between the received signal and the local generated code resides within a fraction of chip duration [4]. Despite the existence of multiple in-phase cells, the conventional acquisition schemes analyzed in [3]–[8] have been first developed under the assumption that there exists only one in-phase cell. The effects of multiple in-phase cells on the performance of conventional acquisition schemes are investigated in [4] and [8]. Recently, there have been a few attempts to utilize multipaths for acquisition performance improvement in frequency-selective fading channels. In [9], a conventional serial search scheme with joint twin-cell detection has been proposed to improve serial acquisition performance. In [10], the optimal decision rule has been developed using the maximum-likelihood estimation technique to improve parallel acquisition performance.

The objective of this paper is to propose a new serial acquisition scheme which can effectively utilize multipaths to improve acquisition performance in frequency-selective fading channels. The effective utilization of multipaths may become more important in next generation DS/SS systems, where wide bandwidths are employed to provide high date rate services [1], [2], resulting in an increase in the number of resolvable paths. In a conventional serial acquisition scheme, cells in an uncertainty region are tested consecutively and the test is performed by cell-by-cell detection [3], [4]. This scheme is appropriate if there is only one in-phase cell [3]. In frequency-selective fading channels, however, there may exist a number of in-phase cells, whose code phase differences are less than the delay spread [4]. To exploit the presence of more than one in-phase cells, the use of nonconsecutive search is proposed in this paper. The nonconsecutive search is utilized to decrease the search time by testing cells in a nonconsecutive manner with a step size greater than one chip. Furthermore, the joint triple-cell detection is employed to utilize adjacent cells for a more reliable decision. This scheme may be viewed as an extension of the joint twin-cell detection in [9]. In this detection scheme, neighboring two cells as well as the cell under the test are utilized to perform a test on a cell.

The performance of the proposed acquisition scheme, which employs a nonconsecutive search and joint triple-cell detection, is analyzed in frequency-selective Rayleigh fading channels.

Paper approved by Z. Kostic, the Editor for Wireless Communication of the IEEE Communications Society. Manuscript received February 22, 2000; revised July 2, 2000. This work was supported by the Brain Korea 21 Project. This paper was presented in part at the 11th IEEE Symposium on Personal, Indoor and Mobile Radio Communications (PIMRC 2000), London, U.K., September 2000.

The authors are with the School of Electrical and Computer Engineering, Seoul National University, Seoul 151-742, Korea (e-mail: osshin@mobile.snu.ac.kr; klee@snu.ac.kr).

Publisher Item Identifier S 0090-6778(01)03133-6.

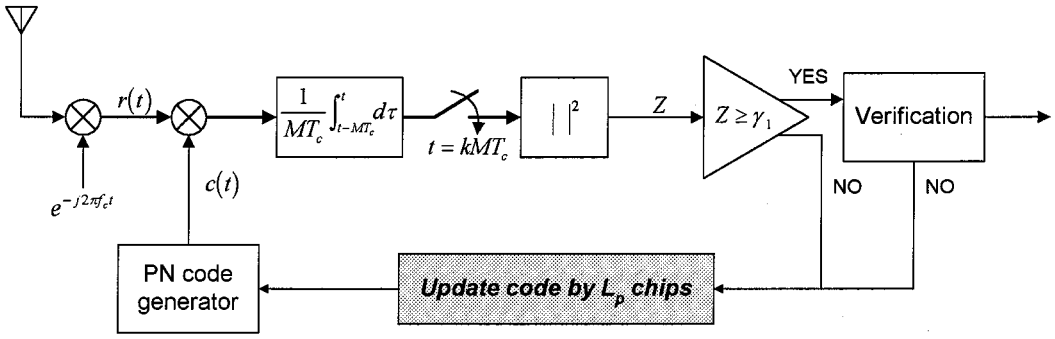

Fig. 1. Structure of an acquisition receiver employing the nonconsecutive search and cell-by-cell detection (NCS-CC).

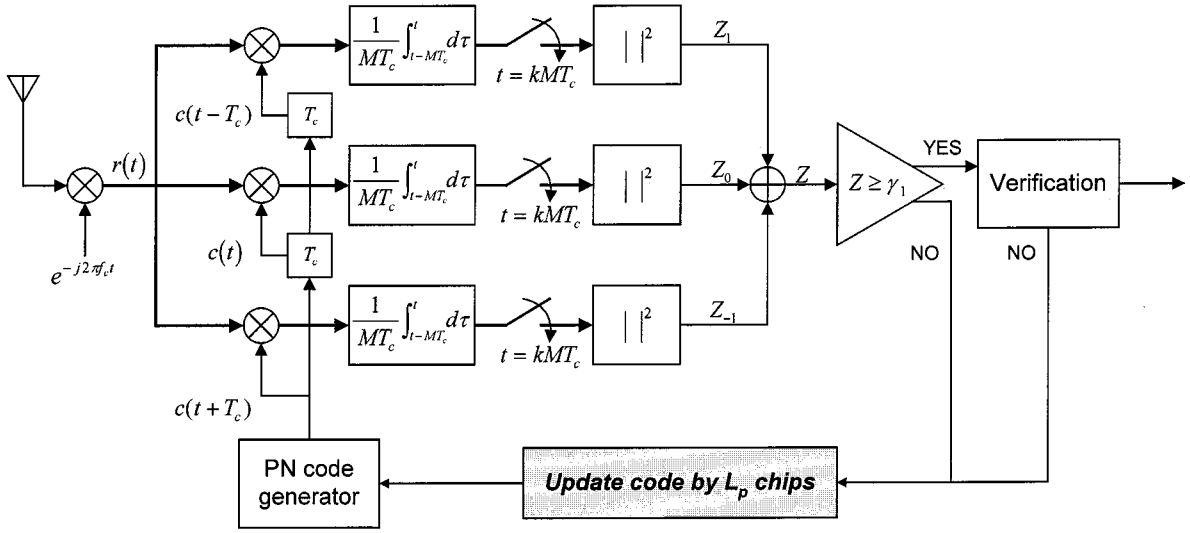

Fig. 2. Structure of an acquisition receiver employing the nonconsecutive search and joint triple-cell detection (NCS-TC).

To investigate the effects of the nonconsecutive search only without joint triple-cell detection, an acquisition scheme which employs the nonconsecutive search and conventional cell-by-cell detection is also considered. Equations for the probabilities of detection and false alarm are derived for frequency-selective Rayleigh fading channels, and an expression for the mean acquisition time is developed. The mean acquisition time performance of the proposed acquisition scheme is compared with that of the conventional one in various channel environments.

This paper is organized as follows. Section II describes the proposed acquisition system. In Section III, performance analyses of the proposed acquisition schemes are presented. In Section IV, mean acquisition time performance of the proposed and conventional acquisition schemes is evaluated and compared. Finally, conclusions are drawn in Section V.

II. Proposed Acquisition System

A. Acquisition Receiver Structure

The acquisition system proposed in this paper utilizes the presence of more than one resolvable path signals, and is based on a serial search double dwell noncoherent system that has two modes of operation, i.e., search mode and verification mode, as shown in Figs. 1 and 2. In both modes, it is assumed that a DS/SS signal is received without data modulation and a noncoherent detector with an active correlator is employed. A decision variable is formed by conventional cell-by-cell detection in Fig. 1, and by joint triple-cell detection in Fig. 2. In the search mode, the decision variable is compared with a decision threshold. If the decision variable exceeds the decision threshold, the corresponding cell is assumed tentatively to be an in-phase cell (H_1 cell), and the verification mode is activated to test whether the tentative decision is correct or not. Otherwise, the cell is assumed to be an out-of-phase cell (H_0 cell) and a new cell is tested. In the verification mode, the receiver performs a number of tests by comparing the decision variable with a decision threshold. If at least B out of these A decision variables exceed the new decision threshold, acquisition is declared and the tracking system is enabled. Otherwise, the tentative decision is rejected and the acquisition system goes back into the search mode to test a new cell. Before testing a new cell, the code phase is updated by more than one chip, which makes the search procedure be nonconsecutive. The nonconsecutive search and joint triple-cell detection are described in more detail in the following subsections.

B. Nonconsecutive Search

As mentioned in Section I, more than one H_1 cells may exist in frequency-selective fading channels. In order to exploit the presence of multiple H_1 cells, the nonconsecutive search

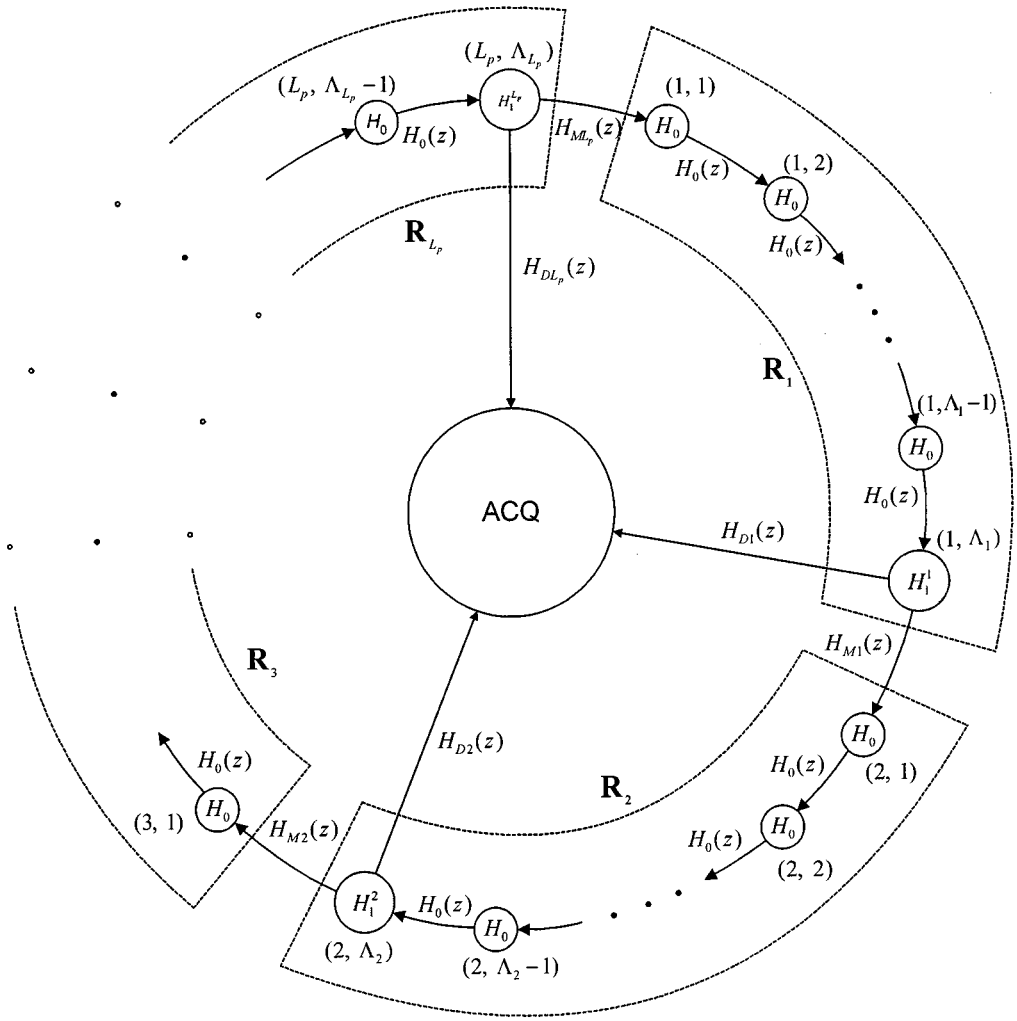

Fig. 3. Circular state diagram of the nonconsecutive search.

strategy is proposed in this paper. In this search strategy, cells in an uncertainty region are tested in a nonconsecutive manner with a step of L_p chips, where L_p denotes the number of resolvable paths, and it is assumed to be known to the receiver. The effect of nonconsecutive search is to test cells in a different order from the conventional consecutive search, so that consecutive H_1 cells are tested nonconsecutively. The nonconsecutive search can be easily implemented by advancing the phase of a local code generator by L_p chips in the code phase update component. The structure of an acquisition receiver employing the nonconsecutive search with cell-by-cell detection is depicted in Fig. 1. In this receiver, only the code phase update component is different compared with a conventional receiver, where only one chip is updated.

The search procedure and benefits of nonconsecutive search may be described by the circular state diagram in Fig. 3. In this figure, the whole uncertainty region which consists of L cells is divided into L_p disjoint subregions $\mathbf{R}_\ell (\ell = 1, 2, \ldots, L_p)$. Λ_ℓ denotes the number of cells in $\mathbf{R}_\ell$. Without loss of generality, the last node (ℓ, Λ_ℓ) in $\mathbf{R}_\ell$ denotes the ℓth H_1 cell (H_1^ℓ cell), which corresponds to the ℓth resolvable path. The other nodes except ACQ denote H_0 cells. In Fig. 3, note that there is one and only one H_1 cell in each subregion, and thus H_1 cells are uniformly distributed over the whole uncertainty region. This reduces time required to reach an H_1 cell from an initial cell, and thus the mean acquisition time may decrease. Another point to be noted is that an additional phase adjustment process of the local code generator is required whenever $\sum_{\ell=1}^{n} \Lambda_{((\ell))}$ cells are tested for $n = 1, 2, 3, \ldots$, where $((\ell)) \triangleq [(\ell - 1) \bmod L_p] + 1$. For example, when $L_p = 3$, the phase should be adjusted whenever the number of tested cells is one of $\{\Lambda_1, \Lambda_1 + \Lambda_2, L, L + \Lambda_1, L + \Lambda_1 + \Lambda_2, 2L, \ldots\}$. This is to avoid the same cell being tested again until all the cells in the uncertainty region are tested.

C. Joint Triple-Cell Detection

In frequency-selective fading channels, the signal power is dispersed into a number of resolvable paths. Therefore, the signal-to-interference ratio (SIR) for each resolvable path decreases with the number of resolvable paths increasing, when the interference power is fixed [10]. In this case, a decision variable formed by conventional cell-by-cell detection may be unreliable compared to a decision variable where the total signal power is contained in a single path. A simple way to increase reliability may be to increase a correlation interval. In real environments, however, the increase in the correlation

interval may degrade acquisition performance due to Doppler spread as well as an increase in dwell time [3], [4]. A joint twin-cell detection scheme has been proposed in [9], where a decision variable is formed by combining detector outputs corresponding to two successive cells. This may increase reliability without increase in the correlation interval. In [10], a similar method has been presented, in which detector outputs corresponding to L_p successive cells are combined to form a decision variable. These detection schemes may be viewed as attempts to improve reliability by utilizing a path diversity technique.

In the joint twin-cell detection scheme in [9], the cell under the test and the previous cell are combined to form a decision variable. In this paper, joint triple-cell detection is proposed as an extension of the joint twin-cell detection. In the joint triple-cell detection, three cells are utilized to form a decision variable: the cell under the test, the previous cell and the next cell. When the number of resolvable paths is greater than three, greater combining gain may be obtained by utilizing three cells instead of two cells. The rationale for the use of both the previous and next cells in combining rather than two previous or two next cells is as follows. When the cell under the test is an H_1 cell, the previous and next cells have an equal probability of being another H_1 cell, and this probability is greater than the probability that the second previous cell or the second next cell is an H_1 cell. Hence, the use of both the previous and next cells are more advantageous than that of two previous or two next cells.

The joint triple-cell detection can be easily implemented using two delay elements without an additional code generator. The structure of an acquisition receiver employing the nonconsecutive search and joint triple-cell detection is shown in Fig. 2. In this figure, Z_0 denotes a detector output corresponding to the cell under the test. Z_{-1} and Z_1 denote detector outputs corresponding to the previous and next cells, respectively. A decision variable Z is formed by combining these three detector outputs: $Z = Z_{-1} + Z_0 + Z_1$.

III. Performance Analysis

In this section, the performance of the acquisition schemes described in Section II is analyzed in frequency-selective Rayleigh fading channels. Two new acquisition schemes, one employing nonconsecutive search and cell-by-cell detection (NCS-CC) and the other employing nonconsecutive search and joint triple-cell detection (NCS-TC), are considered. These two schemes are respectively depicted in Figs. 1 and 2. In Section III-A, the channel model used in performance analysis is presented. In Section III-B, equations for the probabilities of detection and false alarm are derived for NCS-CC and NCS-TC, respectively. In Section III-C, an expression for the mean acquisition time is derived using the circular state diagram in Fig. 3, which is applicable to both NCS-CC and NCS-TC.

A. Channel Model

The channel is modeled as a tapped delay line with tap spacing of one chip [10]. Assuming that fading for each resolvable path is constant over the correlation interval, each tap is multiplied by an independent complex Gaussian random variable. The amplitude and phase of the fading for the ℓth resolvable path are respectively represented as α_ℓ and θ_ℓ, where α_ℓ is a Rayleigh random variable and θ_ℓ is a uniform random variable over $[0, 2\pi)$. The multipath intensity profile (MIP) is assumed to be either uniform or exponentially decaying with the decay rate μ. When the total fading power in all of the resolvable paths is normalized to unity, the average fading power in each resolvable path is represented as [10]

$$E[\alpha_\ell^2] = \begin{cases} 1/L_p, & \mu = 0 \\ \dfrac{1-e^{-\mu}}{1-e^{-\mu L_p}}\, e^{-(\ell-1)\mu}, & \mu \neq 0 \end{cases} \qquad \ell = 1, 2, \ldots, L_p \tag{1}$$

where $E[\cdot]$ denotes the statistical expectation. The number of resolvable paths L_p is assumed to be greater than two in order to guarantee independence of decision variables in NCS-TC.

B. Probabilities of Detection and False Alarm

The receiver is assumed to be chip-synchronized to the received signal. The code period L is discretized with a step size of one chip, resulting in L cells of the uncertainty region. For NCS-CC, the decision variable is a noncoherent detector output itself, as shown in Fig. 1. In this case, the probability density function (PDF) of the decision variable Z corresponding to the ℓth resolvable path is expressed as [10]

$$f(z|H_1^\ell) = \frac{1}{2\sigma_\ell^2}\, \exp\left(-\frac{z}{2\sigma_\ell^2}\right) \tag{2}$$

where H_1^ℓ denotes an H_1 cell corresponding to the ℓth resolvable path. $2\sigma_\ell^2$ denotes the first moment of a decision variable, which is composed of signal and interference: $\sigma_\ell^2 = S \cdot E[\alpha_\ell^2] + \sigma_I^2$, where S and σ_1^2 respectively denote the total transmit signal power and interference power, and $E[\alpha_\ell^2]$ is the normalized fading power of the ℓth resolvable path signal and is given in (1). S/σ_I^2 is defined as the total received SIR, which equals to SIR/chip multiplied by the correlation interval in chips, and $S \cdot E[\alpha_\ell^2]/\sigma_I^2$ is the SIR of a detector output corresponding to the ℓth resolvable path. Similarly, the PDF of the decision variable which does not correspond to any of the resolvable paths is expressed as

$$f(z|H_0) = \frac{1}{2\sigma_I^2}\, \exp\left(-\frac{z}{2\sigma_I^2}\right). \tag{3}$$

From (2) and (3), the probability of detection $P_{D\ell}(\gamma)$ at the ℓth resolvable path and that of false alarm $P_F(\gamma)$ for a given decision threshold γ is calculated as

$$P_{D\ell}(\gamma) = \exp\left(-\frac{\gamma}{2\sigma_\ell^2}\right), \quad P_F(\gamma) = \exp\left(-\frac{\gamma}{2\sigma_I^2}\right). \tag{4}$$

For NCS-TC, the joint triple-cell detection is utilized as shown in Fig. 2. In this case, the PDF of the decision variable $Z = Z_{-1} + Z_0 + Z_1$ can be easily found using the characteristic

function [10], [11]. Since Z_{-1}, Z_0, and Z_1 are independent central chi-square random variables with two degrees of freedom, the characteristic function of Z may be expressed as [11]

$$\Phi_Z(j\nu) = \prod_{k=-1}^{1} \Phi_{Z_k}(j\nu) = \prod_{k=-1}^{1} \frac{1}{1 - j\nu 2\beta_k^2} \tag{5}$$

where $2\beta_k^2$ is the first moment of Z_k.

Under an H_0 cell, there exists no signal component in Z_{-1}, Z_0, or Z_1, i.e., $\beta_k^2 = \sigma_I^2$ $(k = -1, 0, 1)$, and thus (5) becomes

$$\Phi_Z(j\nu|H_0) = \left(\frac{1}{1 - j\nu 2\sigma_I^2}\right)^3 \tag{6}$$

which is the characteristic function of a central chi-square distribution with six degrees of freedom. Therefore, the corresponding PDF is found as [11]

$$f(z|H_0) = \frac{z^2}{16\sigma_I^6} \exp\left(-\frac{z}{2\sigma_I^2}\right). \tag{7}$$

Using the cumulative distribution function (CDF) of (7), the probability of a false alarm for a given decision threshold γ is calculated as

$$P_F(\gamma) = \exp\left(-\frac{\gamma}{2\sigma_I^2}\right) \sum_{k=0}^{2} \frac{1}{k!} \left(\frac{\gamma}{2\sigma_I^2}\right)^k. \tag{8}$$

The characteristic functions for the decision variables corresponding to the states (1, 1) and $(L_p, \Lambda_{L_p} - 1)$ in Fig. 3 are different from (6), since Z_{-1} corresponds to the last resolvable path in state (1, 1) and Z_1 to the first resolvable path in state $(L_p, \Lambda_{L_p} - 1)$. The effects of these two states are assumed to be negligible since the number of this kind of H_0 states is only two, which is generally much less than the total number of H_0 states. Under this assumption, the characteristic function for any H_0 state is assumed to be as represented in (6) in this paper.

Under an H_1 cell, the characteristic function in (5) can be expressed by the partial fraction expansion [10], from which the PDF is found as follows depending on the shape of the MIP.

1) Uniform MIP ($\mu = 0$): For a uniform MIP, the characteristic function for the decision variable corresponding to the ℓth resolvable path may be expressed as [10]

$$\Phi_Z(j\nu|H_1^\ell) = \begin{cases} \dfrac{a}{1 - j2\nu\sigma_I^2} \\ \quad + \displaystyle\sum_{k=1}^{2} \frac{b_k}{(1 - j2\nu\sigma_1^2)^k}, & \ell = 1, L_p \\ \left(\dfrac{1}{1 - j2\nu\sigma_1^2}\right)^3, & \ell = 2, \ldots, L_p - 1 \end{cases} \tag{9}$$

where $a = 1/(1 - \sigma_1^2/\sigma_I^2)^2$ and $b_k = (-\sigma_I^2/\sigma_1^2)^{2-k}/(1 - \sigma_I^2/\sigma_1^2)^{3-k}$. Taking the inverse transform of (9), the PDF may be expressed as [11]

$$f(z|H_1^\ell) = \begin{cases} \dfrac{a}{2\sigma_I^2} \exp\left(-\dfrac{z}{2\sigma_I^2}\right) + \displaystyle\sum_{k=1}^{2} \\ \quad \cdot \dfrac{b_k z^{k-1}}{(2\sigma_1^2)^k (k-1)!} \exp\left(-\dfrac{z}{2\sigma_1^2}\right), & \ell = 1, L_p \\ \dfrac{z^2}{16\sigma_1^6} \exp\left(-\dfrac{z}{2\sigma_1^2}\right), & \ell = 2, \ldots, L_p - 1. \end{cases} \tag{10}$$

From (10), the probability of detection at the ℓth resolvable path for a given decision threshold γ is found as

$$P_{D\ell}(\gamma) = \begin{cases} a \exp\left(-\dfrac{\gamma}{2\sigma_I^2}\right) + \displaystyle\sum_{k=1}^{2} b_k \\ \quad \cdot \exp\left(-\dfrac{\gamma}{2\sigma_1^2}\right) \sum_{m=0}^{k-1} \\ \quad \cdot \dfrac{1}{m!} \left(\dfrac{\gamma}{2\sigma_1^2}\right)^m, & \ell = 1, L_p \\ \exp\left(-\dfrac{\gamma}{2\sigma_1^2}\right) \displaystyle\sum_{k=0}^{2} \frac{1}{k!} \left(\frac{\gamma}{2\sigma_1^2}\right)^k, & \ell = 2, \ldots, L_p - 1. \end{cases} \tag{11}$$

2) Exponentially Decaying MIP ($\mu \neq 0$): For an exponentially decaying MIP, the characteristic function for the decision variable corresponding to the ℓth resolvable path may be expressed as [10]

$$\Phi_Z(j\nu|H_1^\ell) = \sum_{k=\ell-1}^{\ell+1} \frac{c_{\ell k}}{1 - j2\nu\sigma_k^2} \tag{12}$$

where $c_{\ell k} = \prod_{m=\ell-1, m\neq k}^{\ell+1} 1/(1 - \sigma_m^2/\sigma_k^2)$ and $\sigma_0^2 = \sigma_{L_p+1}^2 = \sigma_I^2$. The corresponding PDF is expressed as [11]

$$f(z|H_1^\ell) = \sum_{k=\ell-1}^{\ell+1} \frac{c_{\ell k}}{2\sigma_k^2} \exp\left(-\frac{z}{2\sigma_k^2}\right) \tag{13}$$

from which the probability of detection at the ℓth resolvable path for a given threshold γ is found as

$$P_{D\ell}(\gamma) = \sum_{k=\ell-1}^{\ell+1} c_{\ell k} \exp\left(-\frac{\gamma}{2\sigma_k^2}\right). \tag{14}$$

C. Mean Acquisition Time

In fading channels, the detector outputs in search and verification modes may be correlated. To make the performance analysis be tractable, the effects of this correlation are assumed to be negligible as in [4] and [12]. Under this assumption, the successive decision variables are not correlated for joint triple-cell detection as well as cell-by-cell detection, when the joint triple-cell detection is incorporated with nonconsecutive search. This is because there is no overlap between cells which are utilized to form successive decision variables, if L_p is greater than two. Hence, the mean acquisition time can be calculated using the

flow graph method in [3]. In the circular state diagram in Fig. 3, the branch gains are expressed as

$$H_0(z) = (1-P_{F1})z^T + P_{F1}(1-P_{F2})z^{(2A+1)T} + P_{F1}P_{F2}z^{(2A+1+J/M)T} \quad (15)$$

$$H_{D\ell}(z) = P_{D1\ell}P_{D2\ell}z^{(2A+1)T}, \qquad \ell = 1, 2, \ldots, L_p \quad (16)$$

$$H_{M\ell}(z) = (1-P_{D1\ell})z^T + P_{D1\ell}(1-P_{D2\ell})z^{(2A+1)T} \qquad \ell = 1, 2, \ldots, L_p \quad (17)$$

where $H_0(z)$ is the gain of the branch connecting any of two successive nodes (ℓ, m) and $(\ell, m+1)$ for $m = 1, 2, \ldots, \Lambda_\ell - 1$ and $\ell = 1, 2, \ldots, L_p$. $H_{D\ell}(z)$ and $H_{M\ell}(z)$ are respectively the gain of the branch connecting the nodes (ℓ, Λ_ℓ) and the ACQ, and that of the branch connecting (ℓ, Λ_ℓ) and $(((\ell+1)), 1)$. In (15)–(17), $T = MT_c$ is defined as the correlation interval or dwell time in the search mode, where T_c is the chip duration and J is the penalty time in chips. The correlation interval in the verification mode is assumed to be $2T$. $P_{D1\ell}$ and $P_{D2\ell}$ denote the probabilities of detection at the ℓth resolvable path in the search and verification modes, respectively. P_{F1} and P_{F2} denote the probabilities of a false alarm in the search and verification modes, respectively. These probabilities can be calculated using (4) for NCS-CC and (8), (11) and (14) for NCS-TC:

$$P_{D1\ell} = P_{D\ell}(\gamma_1),$$
$$P_{D2\ell} = \sum_{j=B}^{A} \binom{A}{j} (P_{D\ell}(\gamma_2))^j (1-P_{D\ell}(\gamma_2))^{A-j} \quad (18)$$
$$P_{F1} = P_F(\gamma_1),$$
$$P_{F2} = \sum_{j=B}^{A} \binom{A}{j} (P_F(\gamma_2))^j (1-P_F(\gamma_2))^{A-j} \quad (19)$$

where γ_1 and γ_2 are decision thresholds in the search and verification modes, respectively.

From the circular state diagram in Fig. 3, the transfer function $H(z|\ell, m)$ from a given initial node (ℓ, m) to the ACQ state is calculated as

$$H(z|\ell, m) = \frac{1}{(1-[H_0(z)]^{L-L_p}H_M(z))} \sum_{j=\ell}^{\ell+L_p-1} \cdot [H_0(z)]^{\sum_{k=\ell}^{j}\Lambda_{((k))}+\ell-m-j} H_D(z, \ell, j) \quad (20)$$

where

$$H_M(z) = \prod_{\ell=1}^{L_p} H_{M\ell}(z)$$
$$H_D(z, \ell, j) = H_{D((j))}(z) \prod_{k=1}^{j-\ell} H_{M((j-k))}(z) \quad (21)$$

and Λ_ℓ is given as

$$\Lambda_\ell = \begin{cases} \lfloor L/L_p \rfloor + 1, & 1 \le \ell \le L - \lfloor L/L_p \rfloor L_p \\ \lfloor L/L_p \rfloor, & L - \lfloor L/L_p \rfloor L_p < \ell \le L_p \end{cases} \quad (22)$$

where $\lfloor x \rfloor$ denotes the integer part of x. Under the assumption that the initial code phase of the received signal is uniformly distributed on the whole uncertainty region, the generating function $H(z)$ is found as

$$H(z) = \frac{1}{L}\sum_{\ell=1}^{L_p}\sum_{m=1}^{\Lambda_\ell} H(z|\ell, m) = \frac{1}{L(1-[H_0(z)]^{L-L_p}H_M(z))} \cdot \left\{ \sum_{\ell=1}^{L_p}\sum_{m=1}^{\Lambda_\ell}\sum_{j=\ell}^{L_p+\ell-1} [H_0(z)]^{\sum_{k=\ell}^{j}\Lambda_{((k))}+\ell-m-j} \cdot H_D(z, \ell, j) \right\}. \quad (23)$$

The corresponding mean acquisition time may be calculated as [3]

$$E[T_{\mathrm{ACQ}}] = \left.\frac{dH(z)}{dz}\right|_{z=1} \quad (24)$$

which yields (25), shown at the bottom of the page, where

$$H_M(1) = \prod_{\ell=1}^{L_p} H_{M\ell}(1)$$
$$H'_M(1) = \sum_{\ell=1}^{L_p} \frac{H'_{M\ell}(1)}{H_{M\ell}(1)} \prod_{k=1}^{L_p} H_{Mk}(1)$$
$$H_D(1, j, \ell) = H_{D((j))}(1) \prod_{k=1}^{j-\ell} H_{M((j-k))}(1)$$
$$H'_D(1, j, \ell) = H'_{D((j))}(1) \prod_{k=1}^{j-\ell} H_{M((j-k))}(1) + H_{D((j))}(1) \cdot \sum_{k=1}^{j-\ell} \frac{H'_{M((j-k))}(1)}{H_{M((j-k))}(1)} \prod_{m=1}^{j-\ell} H_{M((j-m))}(1)$$
$$H_{D\ell}(1) = P_{D1\ell}P_{D2\ell}$$
$$H'_{D\ell}(1) = P_{D1\ell}P_{D2\ell}(2A+1)T$$
$$H_{M\ell}(1) = 1 - P_{D1\ell}P_{D2\ell}$$
$$H'_{M\ell}(1) = (1-P_{D1\ell})T + P_{D1\ell}(1-P_{D2\ell})(2A+1)T.$$

$$E[T_{\mathrm{ACQ}}] = \frac{\sum_{\ell=1}^{L_p}\sum_{j=\ell}^{L_p+\ell-1}\left(\sum_{k=\ell}^{j}\Lambda_{((k))} + \ell - j - \Lambda_\ell(\Lambda_\ell+1)/2\right) H'_0(1)H_D(1, \ell, j) + \Lambda_\ell H'_D(1, \ell, j)}{L(1-H_M(1))} + \frac{\sum_{\ell=1}^{L_p}\sum_{j=\ell}^{L_p+\ell-1} \Lambda_\ell H_D(1, \ell, j)((L-L_p)H'_0(1)H_M(1) + H'_M(1))}{L(1-H_M(1))^2} \quad (25)$$

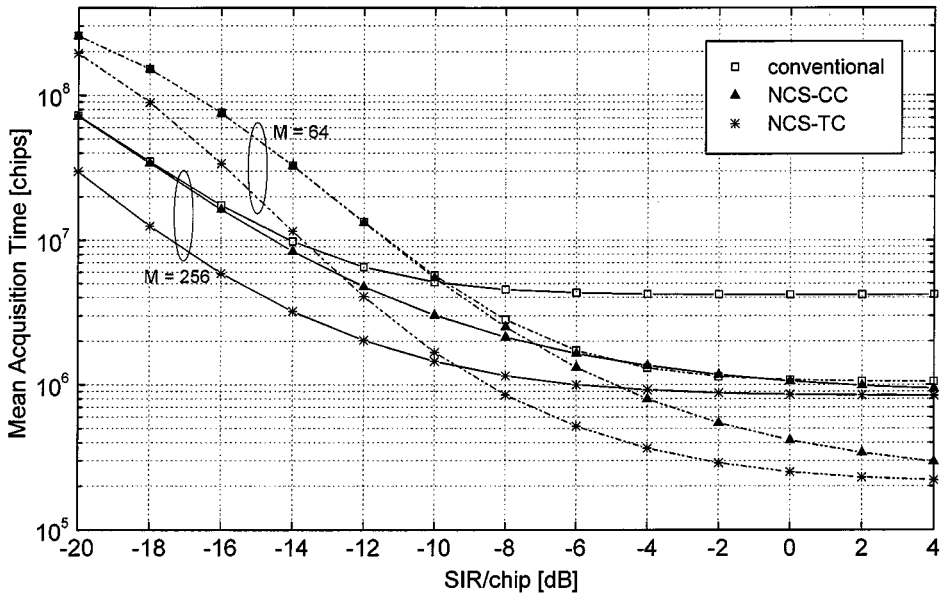

Fig. 4. Mean acquisition time versus SIR/chip ($L_p = 5, \mu = 0$).

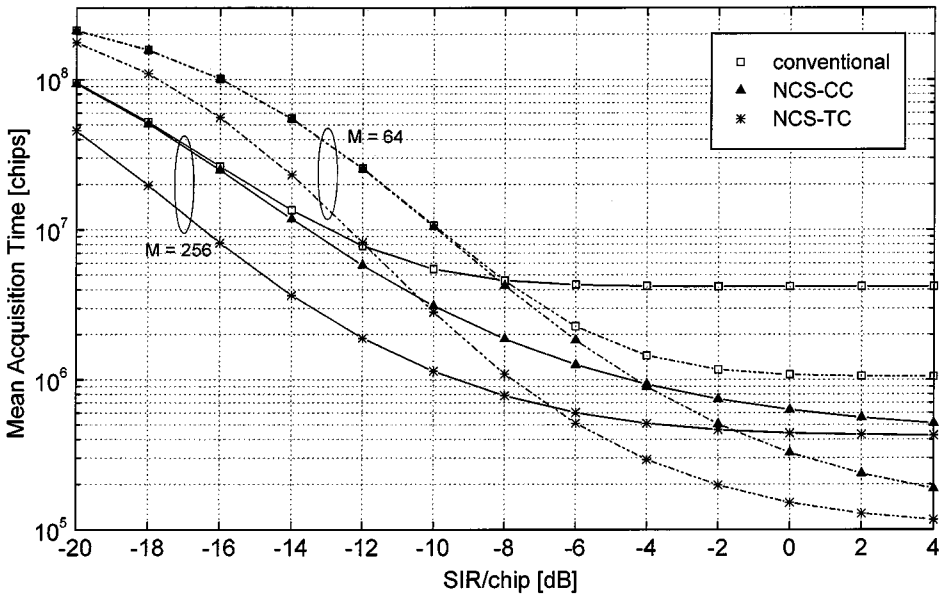

Fig. 5. Mean acquisition time versus SIR/chip ($L_p = 10, \mu = 0$).

$$H_M(1) = \prod_{\ell=1}^{L_p} H_{M\ell}(1)$$

$$H'_M(1) = \sum_{\ell=1}^{L_p} \frac{H'_{M\ell}(1)}{H_{M\ell}(1)} \prod_{k=1}^{L_p} H_{Mk}(1)$$

$$H_D(1, j, \ell) = H_{D((j))}(1) \prod_{k=1}^{j-\ell} H_{M((j-k))}(1)$$

$$H'_D(1, j, \ell) = H'_{D((j))}(1) \prod_{k=1}^{j-\ell} H_{M((j-k))}(1) + H_{D((j))}(1) \cdot \sum_{k=1}^{j-\ell} \frac{H'_{M((j-k))}(1)}{H_{M((j-k))}(1)} \prod_{m=1}^{j-\ell} H_{M((j-m))}(1)$$

$$H'_0(1) = (1-P_{F1})T + P_{F1}(1-P_{F2})(2A+1)T + P_{F1}P_{F2}(2A+1+J/M)T$$

$$H_{D\ell}(1) = P_{D1\ell}P_{D2\ell}$$

$$H'_{D\ell}(1) = P_{D1\ell}P_{D2\ell}(2A+1)T$$

$$H_{M\ell}(1) = 1 - P_{D1\ell}P_{D2\ell}$$

$$H'_{M\ell}(1) = (1-P_{D1\ell})T + P_{D1\ell}(1-P_{D2\ell})(2A+1)T.$$

IV. Performance Evaluation

In this section, the mean acquisition time performance of the proposed acquisition schemes (NCS-CC and NCS-TC) described in Section III are evaluated and compared with that of the conventional one. Equations (18), (19) and (25) are used to calculate the mean acquisition time for NCS-CC and NCS-TC.

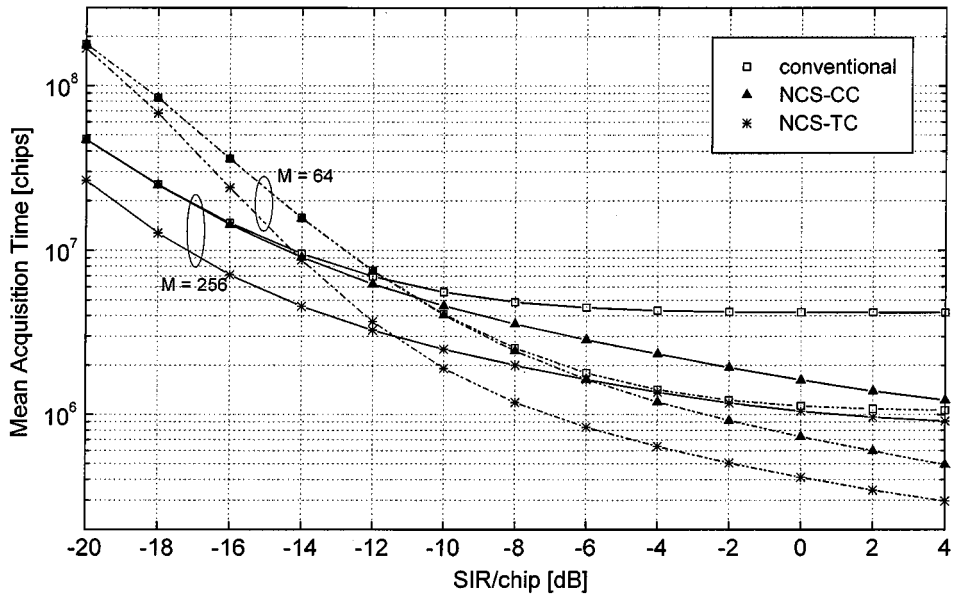

Fig. 6. Mean acquisition time versus SIR/chip ($L_p = 5, \mu = 1$).

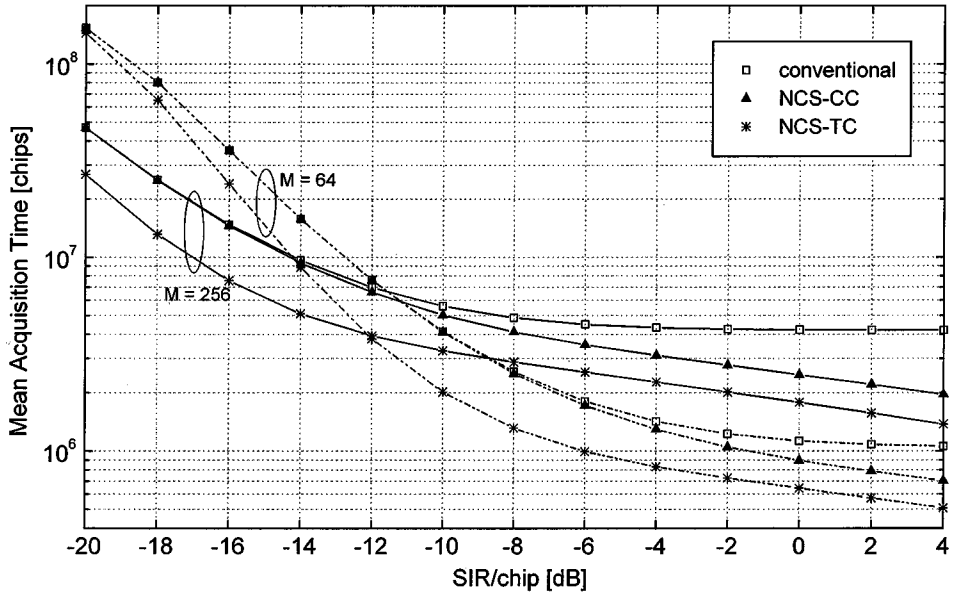

Fig. 7. Mean acquisition time versus SIR/chip ($L_p = 10, \mu = 1$).

The mean acquisition time for the conventional scheme is evaluated using equations presented in [4]. The code period L is set to 2^{15}, and two values of the correlation length M, 64 and 256, are considered in the search mode. As mentioned in Section III, the correlation interval in the verification mode is set two times larger than that in the search mode. As suggested in [3], $A = 4$ and $B = 2$ are chosen for the verification mode, and the penalty factor J is assumed to be 10^5. The decision thresholds γ_1 and γ_2 are determined numerically to minimize the mean acquisition time for each value of SIR/chip.

Figs. 4 and 5 show the mean acquisition time for a uniform MIP, when $L_p = 5$ and $L_p = 10$, respectively. The proposed schemes are shown to always outperform the conventional one. By comparing the performance of NCS-CC with that of the conventional one, the performance improvement through the use of nonconsecutive search is found to increase with the SIR. This may be explained using a performance improvement factor which is defined as the ratio of the mean acquisition time of the conventional scheme to that of NCS-CC. The maximum achievable value of this ratio is about L_p as shown in Figs. 4 and 5, and this may be achieved when the SIR is sufficiently high so that there are no false alarms or miss-detections. At a low SIR, a number of miss-detections and false alarms may occur. Thus, H_1 cells may be repeatedly missed such that cells in an uncertainty region are tested several times on the average to complete acquisition. In this case, the benefits of nonconsecutive search decrease since the time required to reach the first H_1 cell from an initial cell becomes negligible compared to the total acquisition time. At low SIR values, the ratio converges to 1, and thus the performance of two schemes becomes indistinguishable. Figs. 6 and 7 show the mean acquisition

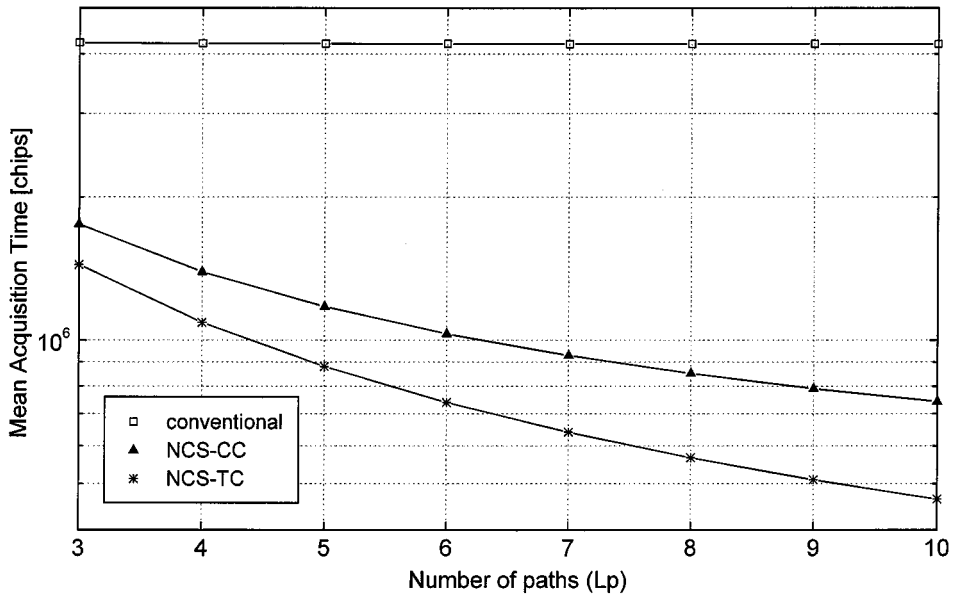

Fig. 8. Effects of the number of resolvable paths on mean acquisition time (SIR/chip $= -2$ dB, $M = 256$, $\mu = 0$).

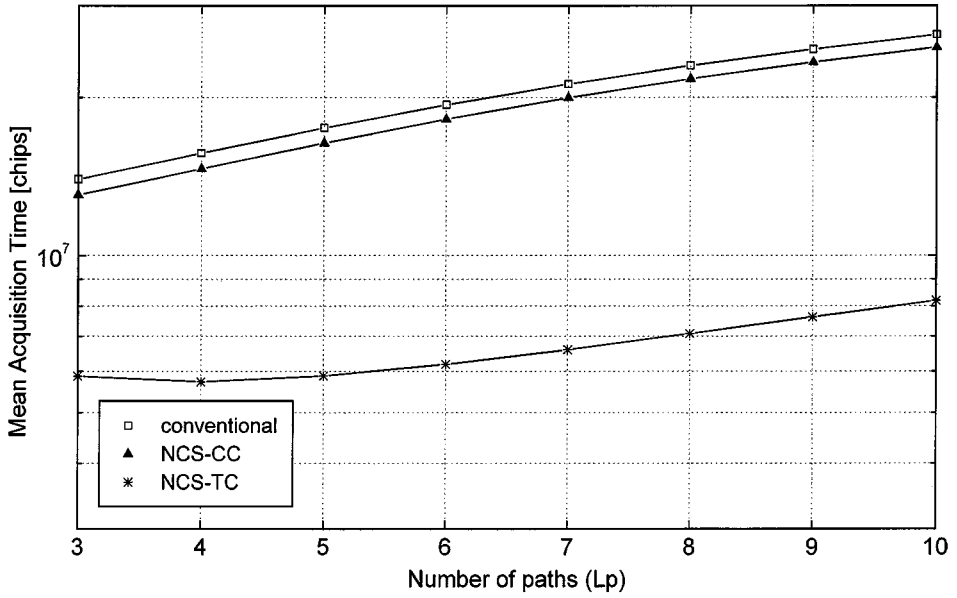

Fig. 9. Effects of the number of resolvable paths on mean acquisition time (SIR/chip $= -16$ dB, $M = 256$, $\mu = 0$).

time for an exponentially decaying MIP with $\mu = 1$, when $L_p = 5$ and $L_p = 10$, respectively. The proposed schemes are observed to outperform the conventional one as in the case of uniform MIP. Comparing Figs. 4 and 6, the performance improvement is found to be greater for a uniform MIP than for an exponentially decaying MIP with $\mu = 1$. This can also be observed from Figs. 5 and 7.

The performance improvement due to joint triple-cell detection is examined by comparing the performance of NCS-CC and NCS-TC. From Figs. 4–7, the use of joint triple-cell detection is found to provide substantial performance improvement for both uniform MIP and an exponentially decaying MIP with $\mu = 1$, especially in a low SIR range. This indicates that the use of joint triple-cell detection effectively mitigates the effects of a decrease in the SIR for each H_1 cell. From Figs. 4–7, for the joint triple-cell detection, the combining gain of a uniform MIP is also higher than that of an exponentially decaying MIP with $\mu = 1$.

The effects of the number of resolvable paths L_p on the mean acquisition time are shown in Figs. 8 and 9 for a uniform MIP and $M = 256$. Fig. 8 is associated with SIR/chip $= -2$ dB, which represents a relatively high SIR, and Fig. 9 with SIR/chip $= -16$ dB, which represents a relatively low SIR. In Fig. 8, the mean acquisition time of NCS-CC and NCS-TC is shown to decrease with L_p increasing, while that of the conventional scheme does not vary with L_p. This indicates that the increase in the number of H_1 cells is more significant than the decrease in SIR for each H_1 cell at SIR/chip $= -2$ dB. In Fig. 9, the performance of NCS-TC is found to improve slightly when L_p changes from 3 to 4, while it degrades, when L_p is higher than 4. The performance of the conventional scheme and NCS-CC is observed to degrade, when increasing L_p. This is because that

the decreasing in the SIR for each resolvable path is more significant than the increasing in the number of H_1 cells. From Figs. 8 and 9, it can also be observed that NCS-TC provides significant performance improvement compared to the conventional scheme for a given range of L_p, whether SIR/chip is high or low.

V. Conclusions

In this paper, an acquisition scheme that effectively utilizes multipaths is proposed in frequency-selective fading channels. This scheme utilizes nonconsecutive search and joint triple-cell detection. Mean acquisition time performance is analyzed in frequency-selective Rayleigh fading channels. The performance of the proposed and conventional acquisition schemes is evaluated and compared. It is found that the proposed acquisition scheme significantly outperforms the conventional schemes over frequency-selective Rayleigh fading channels. The minimum mean acquisition time, which can be achieved at high SIR's, is shown to decrease with the increasing of the number of resolvable paths by employing nonconsecutive search. At a low SIR, the proposed acquisition scheme is also shown to provide a significant performance improvement due to the combining gain provided by the joint triple-cell detection.

References

[1] *UTRA radio transmission technology proposal*, ETSI SMG2, Jan. 1998.

[2] *Introduction to cdma2000 standards for spread spectrum systems*, TIA/EIA/IS-2000.1 TR-45, Mar. 1999.

[3] A. Polydoros and C. L. Weber, "A unified approach to serial search spread-spectrum code acquisition—Parts I and II," *IEEE Trans. Commun.*, vol. COM-32, pp. 542–561, May 1984.

[4] B. B. Ibrahim and A. H. Aghvami, "Direct sequence spread spectrum matched filter acquisition in frequency-selective Rayleigh fading channels," *IEEE J. Select. Areas Commun.*, vol. 12, pp. 885–890, June 1994.

[5] L. B. Milstein, J. Gevargiz, and P. K. Das, "Rapid acquisition for direct sequence spread-spectrum communications using parallel SAW convolvers," *IEEE Trans. Commun.*, vol. COM-33, pp. 593–600, July 1985.

[6] E. A. Sourour and S. C. Gupta, "Direct-sequence spread-spectrum parallel acquisition in a fading mobile channel," *IEEE Trans. Commun.*, vol. 38, pp. 992–998, July 1990.

[7] E. A. Sourour and S. C. Gupta, "Direct-sequence spread-spectrum parallel acquisition in nonselective and frequency-selective Rician fading channels," *IEEE J. Select. Areas Commun.*, vol. 10, pp. 535–544, Apr. 1992.

[8] R. R. Rick and L. B. Milstein, "Parallel acquisition in mobile DS-CDMA systems," *IEEE Trans. Commun.*, vol. 45, pp. 1466–1476, Nov. 1997.

[9] L.-L. Yang and L. Hanzo, "Serial acquisition techniques for DS-CDMA signals in frequency-selective multi-user mobile channels," in *Proc. IEEE Vehicular Technology Conf.*, Houston, TX, May 1999, pp. 2398–2402.

[10] R. R. Rick and L. B. Milstein, "Optimal decision strategies for acquisition of spread-spectrum signals in frequency-selective fading channels," *IEEE Trans. Commun.*, vol. 46, pp. 686–694, May 1998.

[11] J. G. Proakis, *Digital Communications*, 3rd ed. New York: McGraw-Hill, 1995.

[12] W. Zhuang, "Noncoherent hybrid parallel PN code acquisition for CDMA mobile communications," *IEEE Trans. Veh. Technol.*, vol. 45, pp. 643–656, Nov. 1996.

Oh-Soon Shin (S'00) was born in Andong, Korea, in 1975. He received the B.S. and M.S. degrees in electrical engineering from Seoul National University, Seoul, Korea, in 1998 and 2000, respectively.

He is currently working toward the Ph.D. degree in electrical engineering at Seoul National University. His current research interests include mobile communications, spread spectrum communication systems, synchronization, and signal processing for communications.

Kwang Bok (Ed) Lee (M'90) received the B.A.Sc. and M.Eng. degrees from the University of Toronto, Toronto, ON, Canada, in 1982 and 1986, respectively, and the Ph.D. degree from McMaster University, Canada, in 1990.

He was with Motorola Canada from 1982 to 1985, and Motorola USA from 1990 to 1996 as a Senior Staff Engineer. At Motorola, he was involved in the research and development of wireless communication systems. He was with Bell-Northern Research, Canada, from 1989 to 1990. In March 1996, he joined the School of Electrical Engineering, Seoul National University, Seoul, Korea. Currently he is an Associate Professor and Vice Chair in the School of Electrical Engineering, Seoul National University. He has been serving as a Consultant to a number of wireless industries. His research interests include mobile communications, communication theories, spread spectrum, and signal processing. He holds ten U.S. patents and one Korean patent, and has two U.S. patents and five Korean patents pending.